Environ. Sci. Technol. **2000**, *34,* 3982−3990

Photooxidation Pathway of Sulforhodamine-B. Dependence on the Adsorption Mode on TiO_2 Exposed to Visible Light Radiation

GUANGMING LIU, XIANGZHONG LI, AND JINCAI ZHAO*

The Laboratory of Photochemistry, Center for Molecular Science, Institute of Chemistry, The Chinese Academy of Sciences, Beijing 100080, China

HISAO HIDAKA

Frontier Research Center for the Earth Environment Protection, Meisei University, 2-1-1 Hodokubo, Hino, Tokyo 191, Japan

NICK SERPONE

Department of Chemistry and Biochemistry, Concordia University, Montreal, Canada H3G 1M8

The temporal course of the photooxidation of sulforhodamine-B (SRB) in aqueous media illuminated by visible wavelengths in the presence of TiO_2 has been examined to determine the nature of the intermediate species produced and to explore the operative reaction pathway(s). Two pathways are described to account for the differences in the final photooxidation products whose nature depends on the different modes of adsorption of the dye on the metal-oxide mediator. In the SRB/TiO_2 system, when SRB is adsorbed on the positively charged TiO_2 particle surface through a sulfonate group cleavage of the SRB chromophore structure predominates and *N*-de-ethylation occurs only to a slight extent with the major photooxidation products being diethylamine and carbon dioxide. In the presence of the anionic dodecylbenzenesulfonate surfactant DBS, when SRB is near the negatively charged DBS/TiO_2 interface through the positive diethylamine group *N*-de-ethylation occurs preferentially before destruction of the structure with the major products being acetaldehyde and carbon dioxide.

Introduction

The photooxidation of organic compounds on TiO_2 particle surfaces has been examined extensively and is being exploited widely to mineralize a variety of environmentally harmful organic compounds. Typically, the process is initiated by band-to-band excitation of the TiO_2 particles by ultraviolet radiation (*1*−*4*) to generate $^{\bullet}OH$ radicals derived from valence band hole oxidation of terminal OH^- groups and water of hydration on the particle surface. These radicals have been postulated as the dominant oxidizing agents which appear to control the overall kinetics of the oxidative process (*5*, *6*). However, the photocatalytic activity of TiO_2 is limited to irradiation wavelengths in the UV region, thereby limiting effective utilization of solar energy to about 3−5% of the total solar spectrum.

Textile and industrial dyes are becoming one of the largest groups of chemicals manufactured and of consequence are causing significant, albeit progressive pollution to groundwaters in China and the rest of the world (*7*, *8*). Effective utilization of visible sunlight to degrade colored compounds (e.g. dyestuffs) in the presence of TiO_2 particulates promises to be a novel and favorable approach with significant implications to energy resources and environmental remediation (*9*−*13*). The adsorbed dyes are excited by visible light to produce excited states, ^{1,3}dye*, which under suitable circumstances are poised to inject electrons into the semiconductor particle to generate the dye radical cation, dye$^{\bullet+}$. Subsequent transformation of dye$^{\bullet+}$ results in the destruction of the dye chromophore structure and in the formation of small decomposed fragments after a series of complex oxidative steps.

This study examines the photooxidative transformation of the laser dye sulforhodamine-B (SRB) chosen as a prototype molecule because of its high solubility in water and its strong adsorption on the TiO_2 particle surface owing to two possible functions which interact with the positive particle surface under the prevailing conditions used, namely the diethylamine group (positively charged) and the sulfonate group (negatively charged) located at different ends of the dye molecule. Consequently, with the local molecular microenvironment of the SRB dye, adsorption on the TiO_2 surface can easily be changed by simple control of the experimental conditions. The process of photooxidation of SRB in aqueous TiO_2 dispersions under visible illumination is rather complex involving many aspects, such as (i) electron transfer occurring between the excited dye and the conduction band of TiO_2, (ii) formation of radical cations after the electron transfer event, and (iii) hydrolysis or deprotonation of the dye radical cations, among others. These processes are usually affected by the surrounding environment and are closely related to the mode of adsorption. Consequently, the different adsorption modes of SRB are likely to manifest differences in the photooxidative pathways. In this study, UV−visible, COD_{Cr} measurements, ^{1}H NMR, infrared, and GC/MS techniques were brought to bear on defining the mechanism(s) of photooxidation of SRB in aqueous TiO_2 dispersions under visible light illumination. We show that there are two different photooxidation pathways, each of which leads to different photooxidation products; these arise from the two different adsorption modes of the substrate on the metal-oxide mediator.

Experimental Section

Materials. P-25 TiO_2 (ca. 80% anatase, 20% rutile; BET area, ca. 50 $m^2\ g^{-1}$) was kindly supplied by Degussa Co. The spin-trap reagent 5,5-dimethyl-1-pyrroline-*N*-oxide (DMPO) was procured from Sigma Chemical Co. The dye sulforhodamine-B (SRB) was of laser grade quality (Across Co.). The surfactant sodium dodecylbenzenesulfonate (DBS) and all other chemicals were of analytical reagent grade quality and were employed without further purification. Deionized and doubly distilled water was used throughout. The pH of the solution was adjusted with either dilute HCl or NaOH (the original pH of the dye solution was ca. 4.0). The structure of the SRB molecule is illustrated below; the small letters identify the protons for NMR identification.

* Corresponding author fax: +86-10-6487-9375; e-mail: jczhao@ipc.ac.cn. Present address: Institute of Photographic Chemistry, The Chinese Academy of Sciences, Beijing 100101, China.

10.1021/es001064c CCC: $19.00
Published on Web 08/18/2000

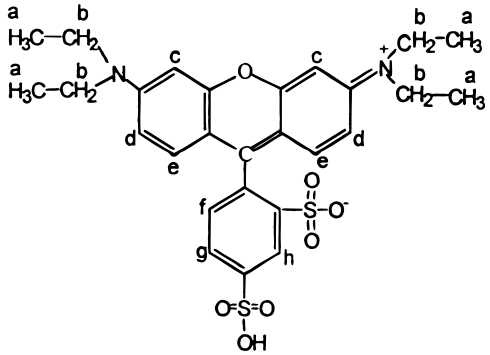

Sulforhodamine B

Photoreactor and Light Source. The visible light source was a 500 W halogen lamp (Institute of Electric Light Source, Beijing) positioned inside a cylindrical Pyrex vessel and surrounded by a circulating water jacket (Pyrex) to cool the lamp and maintain temperature ambient at 298 K and to block unwanted IR radiation. An appropriate cutoff filter was also placed outside the Pyrex jacket to ensure complete removal of radiation below 420 nm and to ensure that irradiation of the SRB/TiO_2 system occurred only by visible light wavelengths. The photon flux of the 500 W halogen lamp at 560 nm was 3.4×10^{-8} einstein s^{-1} as reported earlier (*13c*).

Procedures and Analyses. Aqueous suspensions of SRB (usually 50 mL, 2×10^{-5} M) and 100 mg of TiO_2 particulates were placed in a Pyrex vessel. Prior to irradiation, the suspensions were magnetically stirred in the dark for ca. 30 min to establish an adsorption/desorption equilibrium between the dye and the TiO_2 particle surface. At given intervals of illumination, a sample of the TiO_2 particulates was collected, centrifuged, and then filtered through a Millipore filter (pore size 0.22 μm). The filtrates were analyzed by UV−vis spectroscopy using a Lambda Bio 20 spectrophotometer. Assays of the chemical oxygen demand (COD_{Cr}) was carried out using the potassium dichromate titration method (*14*). The COD_{Cr} of the suspensions (50 mL of 5×10^{-5} M SRB, TiO_2 loading100 mg) was measured directly without removal of the TiO_2 particles at various irradiation time intervals. Ion chromatography (Shimadzu LC-10AS) was used to determine the quantity of $HCOO^-$ ions formed during the photooxidation. Electron paramagnetic resonance (EPR) measurements were carried out at ambient temperature (298 K) using a Bruker ESP 300E spectrometer operating at a microwave frequency of 9.82 GHz and a power level of 5.05 mW; the center field was 3486.7 G and the sweep width was 100.0 G. The modulation amplitude was 1.814 G. Irradiation at $\lambda = 532$ nm was secured from a Quanta-Ray Nd:YAG pulsed (10 Hz) laser system.

Proton NMR spectra were obtained with a Varian 300 nuclear magnetic resonance spectrometer. Samples were prepared as follows: several dispersions containing 200 mL of the SRB dye (1×10^{-4} M) and 400 mg of TiO_2 were irradiated at different time intervals, following which the TiO_2 particles were removed by centrifugation and filtration as described above. Subsequently, the solvent of the filtrate was removed under reduced pressure (below 323 K). The remaining residue was dissolved in 0.5 mL of D_2O. Samples for infrared (IR) spectra (FTS-165 spectrophotometer) were also prepared by a method similar to that for proton NMR, except that the residue was used directly.

The electrochemical redox potential of the SRB/$SRB^{\bullet+}$ couple was measured in water-free acetonitrile media (distilled over P_2O_5) using a Pt working electrode and a Pt counter-electrode; the reference electrode was Ag/AgCl (+0.22 V vs NHE), whereas the supporting electrolyte was 0.1 M $LiClO_4$ dried overnight in a vacuum desiccator. Cyclic voltammograms were obtained on the stationary Pt electrode using an EG&G potentiostat Model 273. The solution in the cell containing 1.0×10^{-3} M SRB was flushed with high-purity nitrogen; temperature was 301 K. The redox potential of the SRB*/$SRB^{\bullet+}$ couple was estimated from $E(SRB^*/SRB^{\bullet+}) = E(SRB/SRB^{\bullet+}) - E^*$.

The intermediate and final products generated during the photooxidative process were analyzed by gas chromatography/mass spectrometric methods (GC-MS, Trio-2000, equipped with a BPX 70 column, size 28 m × 0.25 mm).

Results and Discussion

1. UV−Visible Spectra. The prevailing pH of the solutions can affect the mode and extent of adsorption of SRB on the TiO_2 surface and thus, indirectly, the rate of transformation of the SRB dye; this arises because pH greatly influences the surface charge properties of the metal-oxide particles. The TiO_2 surface is positively charged in acid media (pH below ca. 6.8), whereas it is negatively charged under alkaline conditions (pH greater than 6.8) as evidenced by ζ-potential measurements ($pI_{TiO2} = 6.8$) (*15*). Both the adsorption of SRB and the initial rate of SRB conversion in the SRB/TiO_2 system decreased with an increase in the pH of the dispersion in alkaline media, whereas in acidic media they increased simultaneously with decreasing pH. To better scrutinize the adsorption modes and the photooxidation pathway(s), all the experiments were carried out at pH 2.5 (unless noted otherwise) at which the rate of conversion was greater than at the higher pHs.

The UV−vis spectral changes taking place during the photooxidation of SRB in the SRB/TiO_2 system are illustrated in Figure 1a. The extent of adsorption of the dye (2×10^{-5} M) on TiO_2 (100 mg) particles was ca. 25% (see spectrum 2). Under visible light irradiation, the characteristic absorption band of SRB at ca. 565 nm decreased rapidly, accompanied by concomitant slight hypsochromic shifts indicating the occurrence of some *N*-de-ethylation during the photooxidation of SRB. These observations are in keeping with similar earlier observations of an electron-transfer reaction in the Rhodamine-B/CdS system (*16*). The color of the dispersion disappeared indicating that at least the chromophoric structure of the dye was destroyed. Absorption spectra revealed no new intermediates or products formed that would have manifested new absorption features in the visible and near-ultraviolet region. Control experiments established that SRB did not degrade in TiO_2 suspensions in the dark or when illuminated with visible light in the absence of TiO_2. Visible light illumination of SRB in the presence of SiO_2 or Al_2O_3 particles, substituted for TiO_2 particulates, caused no dye degradation. We infer from this that both visible light and TiO_2 semiconductor particles are indispensable to the photooxidative conversion of SRB.

The inset to Figure 1a shows the temporal concentration changes of SRB illustrating a first-order exponential fit of the decay with $k = 8.8 \times 10^{-2}$ min^{-1}. That rapid decomposition occurred is consistent with the notion that relatively strong adsorption enhances photooxidation on the TiO_2 surface (*12b*). The tendency of the SRB maximum absorption to blue shift is also illustrated in the inset of Figure 1a. Two competitive processes, namely *N*-de-ethylation and cleavage of the SRB chromophore ring structure, occur concurrently during photooxidation with the latter process predominating (e.g. compare part a with part b of Figure 1).

When the anionic surfactant DBS is added to the SRB/TiO_2 system, de-ethylation predominates during the initial stages (Figure 1b). Destruction of the chromophore ring structure of the fully de-ethylated dye occurred only after ca. 60 min of visible irradiation. Moreover, only 19% of the fully de-ethylated dye was converted after ca. 240 min of further

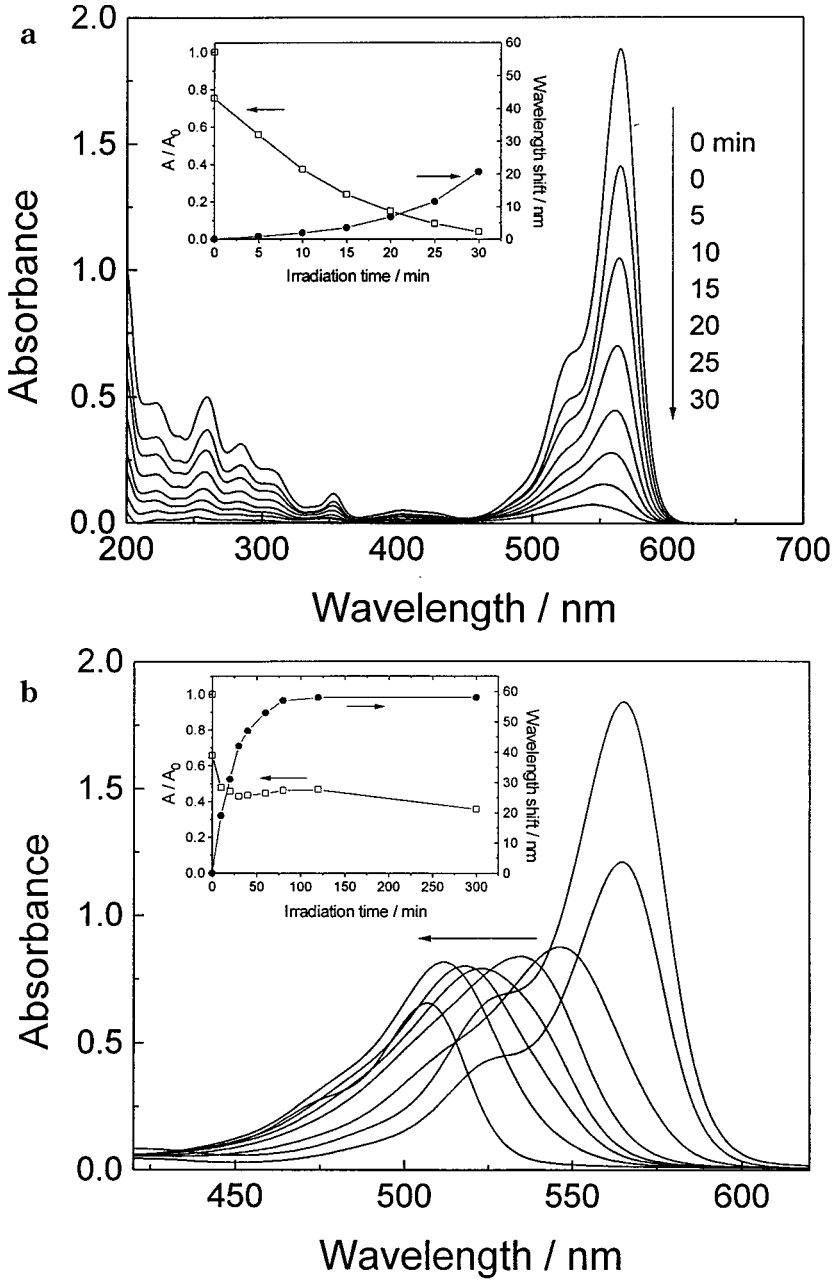

FIGURE 1. (a) UV−visible spectral changes of SRB (2×10^{-5} M, 50 mL) in aqueous TiO_2 dispersions as a function of irradiation time. Spectra from top to bottom correspond to cases where TiO_2 was absent (0 time), after addition of TiO_2 particles (2 g L^{-1}) and achievement of an equilibrium concentration (0 time), followed by irradiation for 5, 10, 15, 20, 25, and 30 min, respectively. Inset: SRB concentration changes and wavelength shifts of the maximal absorption as a function of with irradiation time. (b) UV−visible spectral changes of SRB (2×10^{-5} M, 50 mL) in aqueous TiO_2/DBS (cmc) dispersions with irradiation time. Spectra from right to left refer to those before addition of TiO_2 particles; after addition of TiO_2 particles (2 g L^{-1}) and DBS (1.2 mM) to reach an equilibrium concentration; then followed by irradiation for 10, 20, 30, 40, 60, and 300 min, respectively. Inset: SRB concentration changes and wavelength shifts of the major absorption band with irradiation time.

irradiation (see inset to Figure 1b). Under visible illumination, the dye is de-ethylated in a stepwise manner with the color of the dispersion changing from an initial red color to a light green-yellow (i.e. ethyl groups are removed one by one as confirmed by the gradual peak wavelength shifts toward the blue region, see Figure 1b). The fully de-ethylated SRB molecule has a major absorption band at $\lambda_{max} = 506$ nm, in accord with standard spectra. As expected, the eliminated ethyl groups were oxidized to acetaldehyde (see other results below).

We focus first on the photooxidation process of SRB in the SRB/TiO_2 system to elucidate the mechanistic details of the process under visible light excitation.

2. Chemical Oxygen Demand. Changes in the chemical oxygen demand (COD_{Cr}) of the dispersions reflect the degree to which the dye (or any organic substance) is degraded or mineralized during irradiation. Table 1 summarizes the results of COD_{Cr} measurements. COD_{Cr} values for the irradiated SRB/TiO_2 suspensions decreased with increasing illumination time from an initial value of 42.0 mg O_2 L^{-1} (before illumination) to 11.6 mg O_2 L^{-1} after 12 h of irradiation. Such significant COD_{Cr} changes (72.4%) indicate unambiguously that photooxidation of SRB in the presence of TiO_2 under visible light irradiation is not a simple discoloration or a simple destruction of the chromophoric structure of the dye, because a large number of carbon atoms in the dye

TABLE 1. COD_{Cr} Changes of SRB (50 mL, 5×10^{-5} M) Dispersions (pH = 4.0; TiO_2 Loading, 100 mg) with Irradiation Time

irradiation time (h)	0	1	3	5	7	11	12	14
COD_{Cr}	42.0	34.8	31.2	21.6	17.2	13.2	11.6	11.6
$[COD_0-COD_t]/COD_0$, %	0.0	17.1	25.7	48.6	59.0	68.6	72.4	72.4

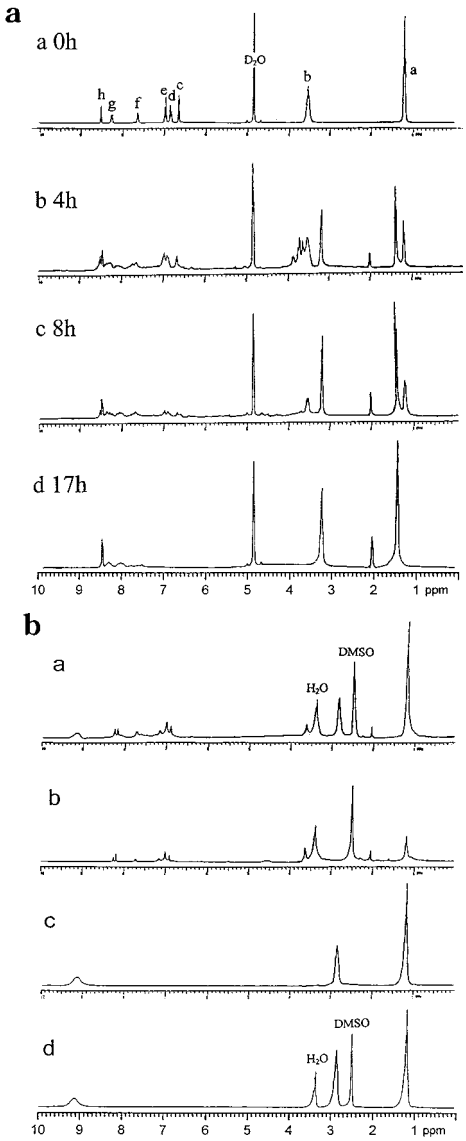

FIGURE 2. (a) Temporal profile of the ^1H NMR spectra at various irradiation intervals during the photooxidation of sulforhodamine-B. (The strong signal at δ 4.85 ppm is that of an impurity, probably water, in the D_2O solvent). (b) (a) ^1H NMR spectrum obtained after 4 h of irradiation of the SRB/TiO_2 dispersion (solvent is DMSO instead of D_2O); (b) spectrum obtained by reduced-pressure distillation of the sample used to record spectrum a under alkaline conditions; (c) spectrum obtained by subtracting spectrum b from spectrum a; (d) spectrum of an authentic diethylamine hydrochloride sample.

molecule are converted to CO_2. Details of the process were further elucidated by ^1H NMR, IR, and GC/MS methods.

3. Proton NMR Spectra. To identify the species produced in the photooxidation of SRB, the temporal proton NMR profiles of the dye, intermediates, and final products were monitored by proton nuclear magnetic resonance spectroscopy. Spectrum **a** in Figure 2a shows the typical proton NMR signals of pure SRB and their assignments to the various protons in the structure of SRB (see above). The NMR signals

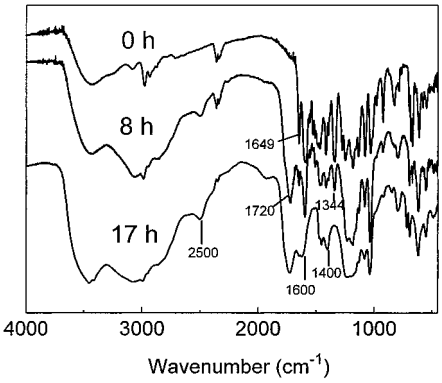

FIGURE 3. Temporal variations in the IR spectra in the photodegradation of SRB under visible light irradiation.

of the aromatic hydrogens H_c, H_d, H_e, H_f, H_g, and H_h are located at δ 6.66, 6.83−6.86, 6.96−6.99, 7.62−7.65, 8.25−8.28, and 8.52 ppm, respectively; those of H_a and H_b of the *N*-diethyl group appear at δ 1.18−1.23 and 3.49−3.60 ppm, respectively. During the course of the photooxidation (spectra **a**−**d** in Figure 2a), a series of new signals appeared at δ 1.30−1.50 ppm (hydrogens from the CH_3 and analogous groups), 2.04 ppm, 3.10−3.30 ppm, and 8.46 ppm, whereas the characteristic signals of SRB at δ 1.18−1.23 ppm (CH_3), δ 3.49−3.60 ppm (CH_2), and δ 6.60−8.60 ppm (aromatic protons) disappeared. The signals at δ 8.46 ppm and δ 2.04 ppm increased with increasing illumination time. We attribute the signal at δ 8.46 ppm to the CH proton of formic acid (confirmed by ion chromatography) and the signal at δ 2.04 ppm to the methyl protons of CH_3CHO (also see the IR and GC-MS results). Of particular relevance are the proton signals at δ 1.30−1.50 ppm (new) and δ 3.10−3.30 ppm (new), together with the methyl (CH_3) protons at δ 1.18−1.23 ppm and the methylene (CH_2) protons at δ 3.49−3.60 ppm of SRB, all of which exhibit peculiar features. The intensities of the two new signals increased with irradiation time, whereas the latter two signals decreased in intensity with time. More interesting is the ratio of the integrated area of the first two peaks which remained constant at 3:2 during the photooxidation, the same as the ratio of the latter two signals. This observation demonstrates that the ethyl group (CH_2CH_3) of SRB is not destroyed in the photooxidation process but rather exists in the final photooxidation products in the form of diethylamine (actually, as diethylamine hydrochloride due to a large quantity of chloride present from adjusting the pH of the original solutions with HCl; also see results in Figure 3 and in Figure 4a below).

On the basis of the signal intensities from proton NMR spectra (spectrum **d** of Figure 2a), we establish that diethylamine is a major photooxidation product in the SRB/TiO_2 system (also see the GC-MS results, Figure 4a). However, the NMR signals of the NH or NH_2 functions of diethylamine were not observed in this system owing to proton exchange between the active proton and the solvent used, D_2O. To further confirm the nature of the principal product, we used DMSO as the solvent in lieu of D_2O (Figure 2b, spectrum **a**; same sample as used to record spectrum **b** of Figure 2a, except for the solvent). The broad peak appearing at δ 9.10−9.20 ppm arises from the nitrogen proton of diethylamine hydrochloride. Because of the nature of DMSO, the signals

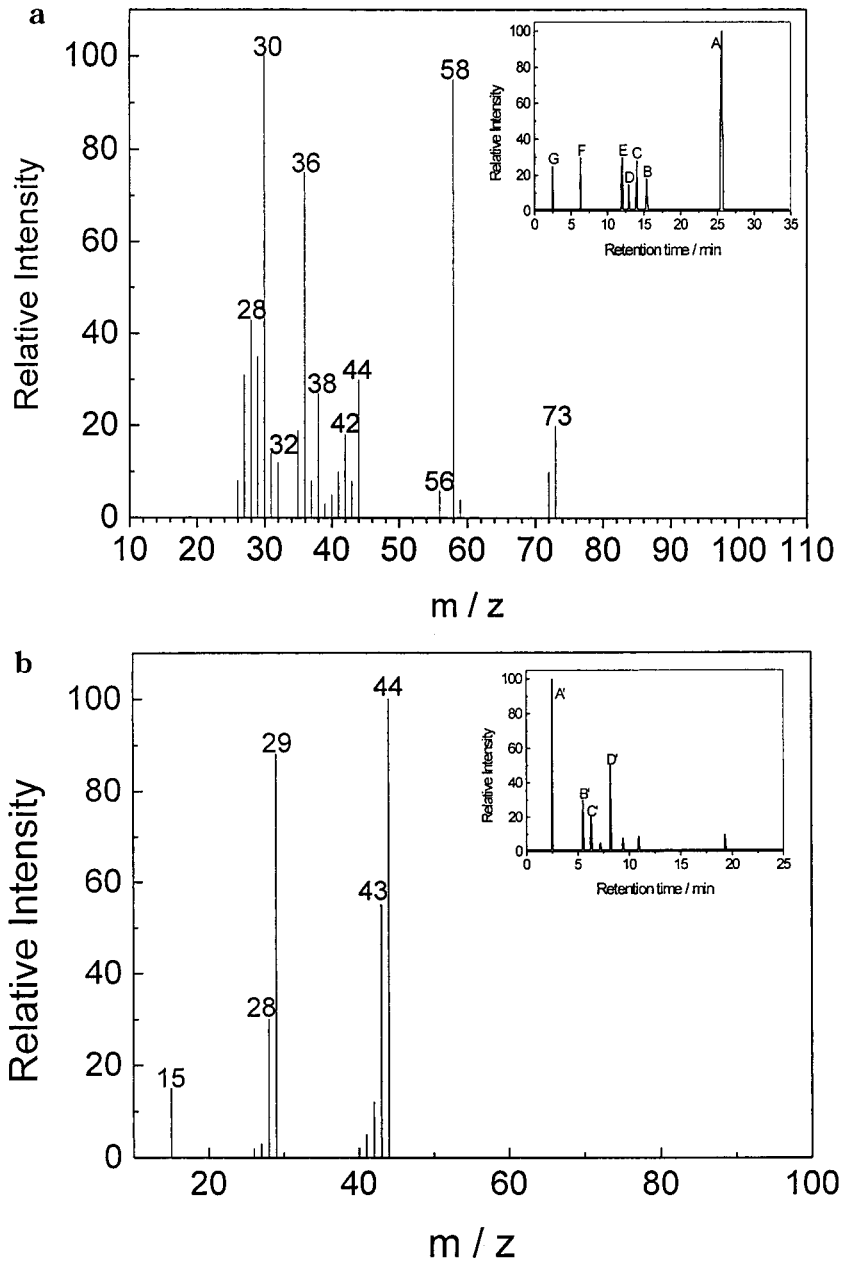

FIGURE 4. (a) Mass spectral data of the major GC component A. Inset: Gas chromatogram of the final photooxidation products of SRB for the adsorption mode involving a sulfonate group. (b) Mass spectral data of the major GC component A′. Inset: Gas chromatogram of the final photooxidation products of SRB for the adsorption mode whereby a diethylamine group is involved in adsorption of SRB to the TiO_2 surface.

of the methyl and methylene protons of SRB were observed at δ 1.10−1.30 ppm and δ 2.70−2.90 ppm, respectively, whereas the signals of the corresponding methyl protons of diethylamine hydrochloride appeared at δ 1.18 ppm, overlapping with those of SRB; the signals of the methylene group protons of diethylamine hydrochloride appeared at δ 3.62 ppm, a location different from that of the corresponding group in the diethylamine/D_2O system.

Distillation of an irradiated aqueous SRB/TiO_2 sample under alkaline conditions (pH = 10.5) led to removal of diethylamine as evidenced by the loss of the corresponding proton NMR signals at δ 9.10−9.20 ppm, δ 3.62 ppm, and δ 1.18 ppm (Figure 2b, spectrum **b**). The proton NMR spectrum of diethylamine hydrochloride (spectrum **c**) can be obtained by subtracting spectrum **b** from spectrum **a** to give a spectrum identical with that of an authentic sample of diethylamine hydrochloride (spectrum **d**).

The above NMR findings support the suggestion made previously that the breakup of the chromophoric structure of SRB dominates during the initial irradiation stage (formation of a large quantity of diethylamine) with only a small extent of de-ethylation taking place as attested by formation of a small quantity of CH_3CHO. This is consistent with the results of Figure 1a and with the adsorption mode (Scheme 1a) whereby the SRB dye is adsorbed on the TiO_2 surface through a sulfonate group.

4. Infrared Spectra. The IR spectra illustrated in Figure 3 were also used to monitor the temporal course of the photoinduced conversion of SRB illuminated by visible irradiation and to provide additional evidence for the operational pathway(s). Results available in the literature (*17*) suggest the following assignments for the principal bands in the IR spectra of SRB (before irradiation): the bands at 1590, 1558, 1530, 1510, 1490, and 1470 cm^{-1} correspond to

SCHEME 1. Proposed Photooxidation Pathways of SRB in Aqueous TiO_2 Dispersions under Visible Light Irradiation: (a) Adsorption Mode with a Sulfonate Group and (b) Adsorption Mode with a Diethylamine Group

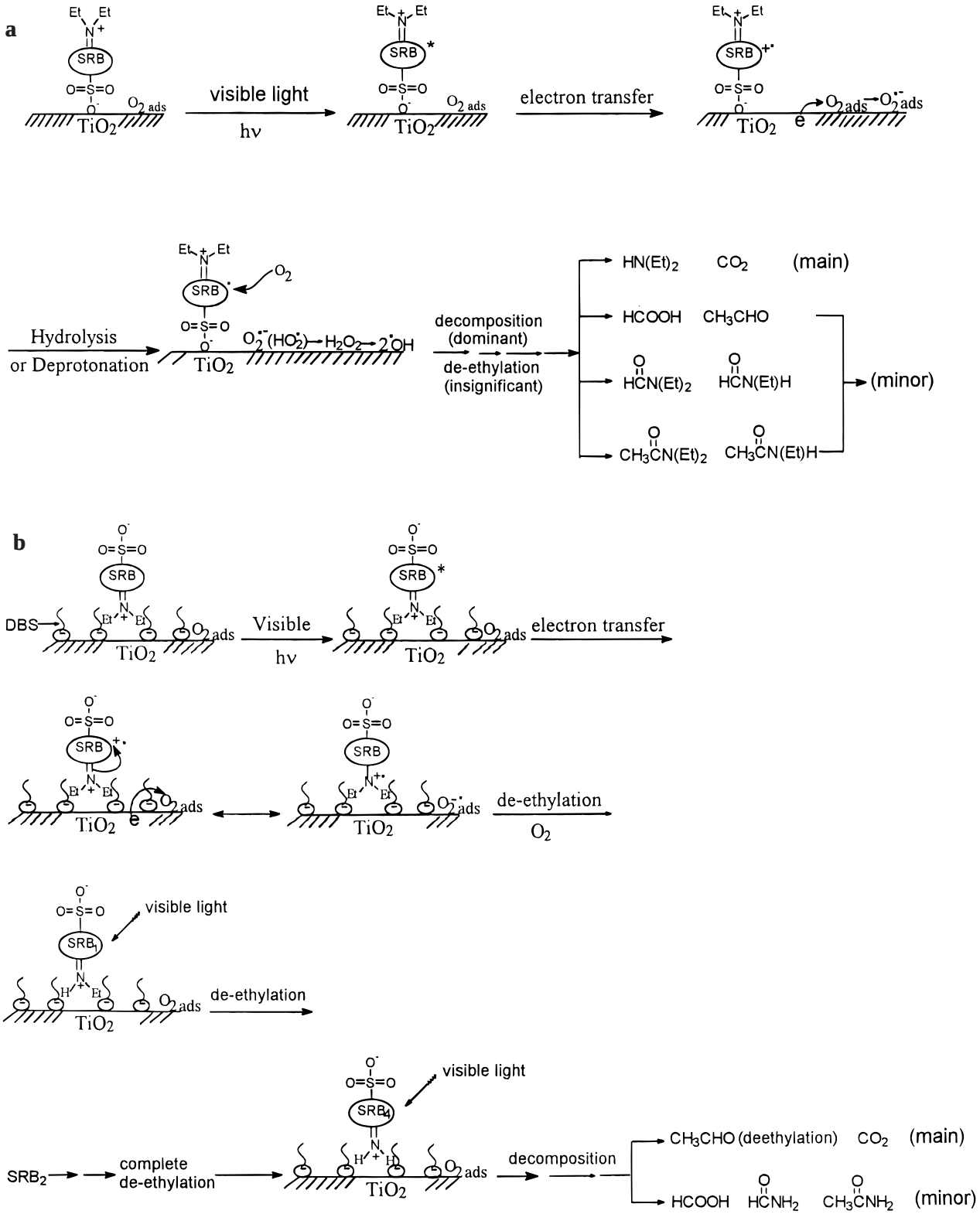

aromatic ring vibrations, whereas the 1344 cm^{-1} band is due to C-aryl bond vibrations. The bands at 1120−1145 cm^{-1} and 668−625 cm^{-1} are caused by vibrations in the $-SO_3^-$ group, whereas the band at 1649 cm^{-1} is attributed to vibrations of the carbon−nitrogen bond and the heterocycle vibrations are the origins of the band at 1530−1558 cm^{-1}. During photooxidation, bands of vibrations characteristic of the carbon−nitrogen bond (1649 cm^{-1}), the C-aryl bond (1344 cm^{-1}), the aromatic ring, and heterocycle vibrations (1470−1590 cm^{-1}) decreased with irradiation time and disappeared after about 17 h of irradiation. At the same time, a strong new IR band appeared at 1720 cm^{-1} attributable to >C=O groups. The IR results indicate convincingly that the large conjugated chromophore structure of SRB is destroyed under visible light irradiation in aqueous media through the mediation of TiO_2 particulates and is further decomposed to

TABLE 2. Positive Ion Mass Spectra of the Final Photooxidation Products of SRB[a]

	A	B	C	D	E	F(C′)	G(A′)	B′	D′
$[M]^+$	73(20%)	87(28%)	73(38%)	115(24%)	101(35%)	46(60%)	44(100%)	45(100%)	59(100%)
$[M - H]^+$						45(50%)	43(55%)	44(25%)	
$[M - CH_3]^+$	58(95%)	72(8%)	58(15%)	100(5%)	86(15%)		29(85%)		44(75%)
$[M - NH_2]^+$								29(30%)	43(65%)
$[M - OH]^+$						29(100%)			
$[M - C_2H_5]^+$	44(30%)		44(22%)	86(4%)	72(8%)				
$[M - C_2H_5N]^+$	30(100%)		30(100%)						
$[M - C_3H_7]^+$				72(17%)	58(63%)				
$[M - C_3H_8]^+$		43(70%)							
$[M - C_3H_7N]^+$		30(100%)							
$[M - C_4H_9]^+$				58(100%)	44(42%)				
$[M - C_4H_9N]^+$					30(100%)				
$[M - C_4H_{10}N]^+$				43(66%)					

[a] The data in brackets represent relative intensities.

smaller organic species containing >C=O groups: e.g. *N*-ethylacetamide, *N*-ethylformamide, *N*,*N*-diethylacetamide, *N*,*N*-diethylformamide, HCOOH, and CH_3CHO, as confirmed by the proton NMR evidence above and by the GC-MS results below. In addition, a series of new IR absorption bands belonging to diethylamine hydrochloride appeared at 3000, 2500, 1600, 1450, 1400 cm^{-1}, in accord with standard IR spectra of an authentic sample.

5. GC-MS Measurements. Further convincing evidence for the operational pathway(s) was obtained by GC-MS spectroscopic methods for the two different systems (see Scheme 1 below), which would likely lead to two different photooxidation pathways as inferred from the results displayed in Figure 1a,b. The GC-MS results of the final photooxidation products for the SRB/TiO_2 system are presented in Figure 4a. The predominant peak **A** in the GC chromatogram (inset to Figure 4a) was analyzed in detail by mass spectroscopy. The major component **A** corresponds to diethylamine (i.e. diethylamine hydrochloride) in accord with results from proton NMR and IR spectroscopy. Mass spectral analyses confirmed that the other (minor) final products were *N*-ethylacetamide (**B**), *N*-ethylformamide (**C**), *N*,*N*-diethylacetamide (**D**), *N*,*N*-diethylformamide (**E**), formic acid (**F**), and acetaldehyde (**G**). The major features of the positive ion mass spectra are summarized in Table 2. Because the amounts of components **B**–**E** are relatively small compared to **A** and because the positions of their NMR signals are similar to those of **A**, their identification was precluded by the ^1H NMR spectral method (Figure 2).

The presence of **B** and **C** indicates that de-ethylation is incomplete, whereas formation of **A** (main product), **D**, and **E** demonstrates that destruction of the chromophore structure is the predominant process in the photooxidation of SRB, in accord with the adsorption mode depicted in Scheme 1a (see below). More important, according to the relative intensity of **A**–**G** in the gas chromatograms it is possible to predict the approximate theoretical changes in the COD values of SRB during its photooxidation (i.e. from the SRB molecule to the final photooxidation products). We obtain ca. 65.4%, in relatively good agreement with the experimental results from COD measurements (72.4%, see Table 1).

Figure 4b illustrates the GC-MS results of the final products of SRB photooxidation in the SRB/DBS/TiO_2 system (Scheme 1b). From the results of mass spectral analysis, we confirmed that the major component **A′** in the gas chromatograms is acetaldehyde (the de-ethylated product, Figure 4b); the other (minor) components are **B′**, formamide; **C′**, formic acid; and **D′**, acetamide. The major features of the positive ion mass spectra are summarized in Table 2. The presence of the products **A′**, **B′**, and **D′** and the absence of **A**–**E** indicate that the *N*-de-ethylation process occurs preferentially before destruction of the structure at this adsorption mode.

6. Initial Photooxidation Pathway. After photoexcitation of the SRB/TiO_2 system at $\lambda > 420$ nm, injection of an electron from the excited dye (^{1,3}dye*) to TiO_2 takes place since the thermodynamics are appropriate {$E(SRB^*/SRB^{\bullet+}) = -1.30$ V vs NHE and $E_{CB}(TiO_2) = -0.5$ V vs NHE (*6*)}; the $TiO_2(e^-)$ is then scavenged by preadsorbed molecular oxygen to yield active oxygen radicals and the cation radicals $SRB^{\bullet+}$. The role of active oxygen radicals produced in the photooxidation of SRB was also examined.

Although the hydroxyl radical was detected as the DMPO–$^\bullet$OH adduct in the EPR measurements, it is not the principal and sole species that leads to photooxidation of SRB in the presence of TiO_2 under visible irradiation. This was confirmed by control experiments. Photooxidation of the dye was not inhibited under conditions otherwise identical to those above except for the presence of 2-propanol (1%), known to be a good $^\bullet$OH radical quencher (*18*). Moreover, when added to the dispersion (SRB: 2×10^{-5} M; TiO_2 loading: 2 g L^{-1}) superoxide dismutase (SOD: 2.5 mg mL^{-1}, activity: 10,000 U mg^{-1}), which catalyzes the disproportionation of $O_2^{\bullet-}$ to H_2O_2 and O_2, had no effect on the initial degradation rate. This precludes any effect of the active superoxide radical species on the photooxidation process.

Surface-adsorbed oxygen plays the important role of scavenging the $TiO_2(e^-)$ electron thereby preventing its recombination with $Dye^{\bullet+}$ (*19*). However, if the exclusive role of O_2 was merely to scavenge the $TiO_2(e^-)$, then the presence of an added oxidizing agent in an O_2-free SRB/TiO_2 dispersion should lead to the same *N*-de-ethylation and photooxidation of SRB on excitation of the surface-adsorbed dye. To test this hypothesis, CrO_4^{2-} was selected as the oxidizing agent (*20*). A 50 mL aqueous dispersion containing SRB (2×10^{-5} M, pH = 4.0), CrO_4^{2-} (1.6×10^{-4} M), and TiO_2 (100 mg) was deoxygenated for 5 h using high purity (99.999%) N_2 gas. The pH of the dispersion was kept at 4.0 to permit CrO_4^{2-} to access the metal oxide surface and scavenge TiO_2 (e^-). Illuminating the dispersion for 5 h with visible light led to negligible degradation in the first 30 min arising from some residual chemisorbed oxygen. After oxygen was totally consumed, no further photooxidation or de-ethylation took place, clearly suggesting an overall inefficiency of CrO_4^{2-} to promote *N*-de-ethylation or photooxidation of the dye. Therefore, the role of molecular oxygen is significant and cannot be substituted in the *N*-de-ethylation and photooxidation of SRB. Consequently, chemisorbed O_2 on the metal-oxide mediator acts not only as an electron trap to suppress $SRB^{\bullet+}/TiO_2$ (e^-) recombination but also as an essential oxidizing agent which participates in the oxidative process leading to de-ethylation and to destruction of the chromophore ring structure, and ultimately to formation of smaller intermediates and CO_2.

In the photooxidation of SRB, different final photooxidation products (as verified experimentally by UV−vis, ^{1}H NMR, IR, and GC-MS) arise, no doubt, from different photooxidation pathways, which are seeming defined by two entirely different adsorption modes. Under our experimental conditions (pH 2.5), the positively charged surface of the TiO_2 particles in the SRB/TiO_2 system permits SRB to be chemisorbed strongly on TiO_2 through the sulfonate groups by electrostatic forces because the presence of two sulfonic acid groups in the dye molecule ensures its existence in the form of a singly charged anion in aqueous solutions within the pH range 2−12 (*17*). When the SRB dye adsorbs on the TiO_2 surface through sulfonate groups then (Scheme 1a), cleavage of the SRB chromophore structure seems to predominate. By contrast, *N*-de-ethylation occurs only to a slight extent. The predominant final products were diethylamine and carbon dioxide. Other (minor) products detected were *N*-ethylacetamide, *N*-ethylformamide, *N*,*N*-diethylacetamide, *N*,*N*-diethylformamide, formic acid, and acetaldehyde (from incomplete de-ethylation).

In a previous study (*15*), we established an adsorption model for the anionic surfactant DBS on the surface of TiO_2 particles at different pHs by measurement of the ζ-potential of TiO_2 particles. Anionic DBS molecules are easily adsorbed on the positively charged TiO_2 surface under acidic conditions (pH 2.5) through the negative sulfonate groups owing to electrostatic effects. This results in a drop of the ζ-potential of TiO_2 particles from 55 mV to −20 mV at the DBS critical micellar concentration of 1.2 mM (cmc). The physical location of the SRB in SRB/DBS/TiO_2 system was evidenced by the fluorescence spectral changes of SRB in different media.

It is well-known that the fluorescence maxima of organic compounds are sensitive to the polarity of the solvent (*21*); that is, the more polar the solvent is the more the fluorescence maximum of the organic compound shifts to the red. When DBS (1.2 mM) was added to an SRB (5×10^{-7} M) solution (pH 2.5), the maximum absorbance of SRB increased suggesting that the presence of DBS helps to separate the aggregated SRB molecules, whereas the red shift of the fluorescence maximum of SRB shows that SRB interacts strongly with DBS; note that the environment formed by DBS is surely more polar than neat water. On the other hand, the maximum absorbance of SRB also shifted red concomitant with SRB fluorescence quenching after addition of colloidal TiO_2 (5×10^{-3} M) to an SRB solution. However, when TiO_2 was added to the SRB/DBS system, except for some fluorescence quenching, there was no shift of the fluorescence maximum of SRB compared with that in the TiO_2-free system. This infers that the SRB molecules are located, to some extent, far from the TiO_2 surface in the SRB/DBS/TiO_2 system (see Scheme 1b), so that the TiO_2 surface has little influence on the shift of the fluorescence maximum of SRB. On addition of the anionic DBS surfactant, it results that the SRB dye can adsorb to the negative TiO_2/DBS interface only through the positively charged diethylamine groups owing to favorable electrostatic interactions.

When the SRB dye molecules are located near the TiO_2 surface through the diethylamine group and assisted by the negative ends of the DBS molecules (cmc: 1.2 mM) (Scheme 1b), which de facto neutralize somewhat the surface, the *N*-de-ethylation process predominates during the initial stages. Destruction of the chromophore ring structure occurs mostly only after full de-ethylation of the dye. The final products were acetaldehyde and carbon dioxide (major products) along with formamide, formic acid, and acetamide as the minor products.

According to earlier reports (*22*−*24*), most oxidative *N*-de-alkylation processes are preceded by formation of nitrogen-centered radical, whereas destruction of dye chromophore structures are preceded by generation of carbon-centered radical (*12*, *13*). Consistent with these, degradation of SRB must occur via two different photooxidation pathways (destruction of the chromophore structure and *N*-de-ethylation) due to formation of different radicals (either carbon-centered radicals or nitrogen-centered radicals). There is no doubt that electron injection from the dye to the conduction band of TiO_2 yields dye cation radicals, a process which is determined by the nature of the HOMO orbitals of the excited dye, ^{1,3}dye*. After this step, the cation radical, dye$^{\bullet+}$, can undergo hydrolysis and/or deprotonation. Because these two processes are sensitive to the molecular surroundings, the question as to which radical is formed (carbon-centered radicals or nitrogen-centered radicals) is dictated by the nature of the different hydrolysis or deprotonation pathways of the dye cation radicals, which in turn are determined by the different adsorption modes of SRB on the TiO_2 particle surface.

On the basis of all the above experimental results (different photooxidation products depend on the different adsorption modes), we tentatively propose the two photooxidation pathways depicted in Scheme 1a,b distinguished by the different adsorption modes. In the first (Scheme 1a), the excited dye in the SRB/TiO_2 system is adsorbed to the particle surface through the sulfonate group. Electron injection to the conduction band of TiO_2 produces the dye radical cations, after which either nucleophilic interactions between SRB$^{\bullet+}$ and H_2O or deprotonation occur to produce neutral carbon-centered radicals. The location of the radical in the otherwise complex dye structure then becomes the point of attack by adsorbed molecular oxygen (see Scheme 1a) leading to a sequence of complex reactions: rapid decomposition via cleavage of the ring rupture and further oxidative reactions to yield a multitude of products. Consequently, cleavage of the SRB chromophore structure predominates with the main products being diethylamine and carbon dioxide; de-ethylation is a smaller process which yields the minor components *N*-ethylacetamide, *N*-ethylformamide, and acetaldehyde.

In the second pathway (Scheme 1b), the dye molecule in the SRB/DBS/TiO_2 system is adsorbed through the positively charged diethylamine function. Following electron injection from the excited dye to the TiO_2 particle surface and subsequent hydrolysis (or deprotonation) yields a nitrogen-centered radical, which is subsequently attacked by molecular oxygen to lead ultimately to de-ethylation. The mono-de-ethylated dye, SRB_1, can also be excited by visible light and be implicated in other similar events (electron injection, hydrolysis or deprotonation, and oxygen attack) to yield a bi-de-ethylated dye derivative, SRB_2. The de-ethylation process as described above continues until formation of the completely de-ethylated dye, SRB_4 (see UV−visible spectral results in Figure 1b). When SRB_4 is excited by visible light, the subsequent transformation of the carbon-centered cation radicals generates formamide, acetamide, and formic acid products as confirmed by the GC-MS results of Figure 4b.

Acknowledgments

The generous financial support of this work from the National Natural Science Foundation of China (No. 29677019, No. 29725715, and No. 29637010), the Foundation of the Chinese Academy of Sciences, and the China National Committee for Science and Technology is gratefully acknowledged. The work in Tokyo is sponsored by a Grant-in-Aid for Scientific Research from the Japanese Ministry of Education (No. 10640569 to H.H.) and in Montreal by a grant from the Natural Sciences and Engineering Research Council of Canada (No. A5443 to N.S.). Finally, the authors thank the reviewers for valuable and useful suggestions on the proposed mechanism.

Literature Cited

(1) Fox, M. A.; Dulay, M. T. *Chem. Rev.* **1993**, *93*, 341.
(2) *Photocatalysis-Fundamentals and Applications*; Serpone, N.; Pelizzetti, E., Eds.;Wiley-Interscience: New York, 1989.
(3) Ollis, D. F.; Pelizzetti, E.; Serpone, N. *Environ. Sci. Technol.* **1991**, *25*, 1522.
(4) Legrini, O.; Oliveros, E.; Braun, A. M. *Chem. Rev.* **1993**, *93*, 671.
(5) Turchi, C. S.; Ollis, D. F. *J. Catal.* **1990**, *122*, 178.
(6) Hoffmann, M. R.; Martin, S. T.; Choi, W.; Bahnemann, D. W. *Chem. Rev.* **1995**, *95*, 69.
(7) Tincher, W. C. *Text. Chem. Color.* **1989**, *21*, 33.
(8) Kulkarni, S. V.; Blackwell, C. D.; Blackard, A. L.; Stackhouse, C. W.; Alexander, M. W. *U.S. Environ. Prot. Agency, Res. Dev. [Rep.]* **1985**, EPA-600/2-85/010.
(9) (a) Vinodgopal, K.; Wynkoop, D.; Kamat, P. V. *Environ. Sci. Technol.* **1996**, *30*, 1660. (b) Nasr, C.; Vinodgopal, K.; Fisher, L.; Hotchandani, S.; Chattopadhya, A. K.; Kamat, P.V. *J. Phys. Chem.* **1996**, *100*, 8436.
(10) Ross, H.; Bendig, J.; Hecht, S. *Solar Energy Mater. Solar Cells* **1994**, *33*, 475.
(11) (a) Zhang, F.; Zhao, J.; Zang, L.; Shen, T.; Hidaka, H.; Pelizzetti, E.; Serpone, N. *J. Mol. Catal. A: Chem.* **1997**, *120*, 173. (b) Zhang, F.; Zhao, J.; Shen, T.; Hidaka, H.; Pelizzetti, E.; Serpone, N. *Applied Catal. B: Environ.* **1998**, *15*, 147. (c) Zhao, J.; Wu, K.; Wu, T.; Hidaka, H.; Serpone, N. *J. Chem. Soc., Faraday Trans.* **1998**, *94*, 673.
(12) (a) Wu, T.; Liu, G.; Zhao, J.; Hidaka, H.; Serpone, N. *J. Phys. Chem. B,* **1998**, *102*, 5845. (b) Zhao, J.; Wu, T.; Wu, K.; Oikawa, K.; Hidaka, H.; Serpone, N. *Environ. Sci. Technol.* **1998**, *32*, 2394.
(13) (a) Wu, T.; Lin, T.; Zhao, J.; Hidaka, H.; Serpone, N. *Environ. Sci. Technol.* **1999**, *33*, 1379. (b) Liu, G.; Wu, T.; Zhao, J.; Hidaka, H.; Serpone, N. *Environ. Sci. Technol.* **1999**, *33*, 2081. (c) Liu, G.; Zhao, J. *New J. Chem.* **2000**, *24*, 411.
(14) Chinese National Standard: GB 11914−89, 1989.
(15) Zhao, J.; Hidaka, H.; Takamura, A.; Pelizzetti, E.; Serpone, N. *Langmuir* **1993**, *9*, 1646.
(16) Watanabe, T.; Takizawa, T.; Honda, K. *J. Phys. Chem.* **1977**, *81*, 1845.
(17) Mchedlov, P. N. O.; Shapovalov, S. A.; Egorova, S. I.; Kleshchevnikova, V. N.; Cordova, E.A. *Dyes Pigm.* **1995**, *28*, 7.
(18) Richard, C. *J. Photochem. Photobiol. A: Chem.* **1993**, *72*, 179.
(19) Vinodgopal, K.; Wynkoop, D. E.; Kamat, P. V. *Environ. Sci. Technol.* **1996**, *30*, 1660.
(20) Fu, H.; Lu, G.; Li, Sh. *J. Photochem. Photobiol. A: Chem.* **1998**, *114*, 81.
(21) Lakowicz, J. R. *Principles of Fluorescence Spectroscopy*; Plenum Press: New York, 1983; Chapter 7, and references therein.
(22) Shaefer, F. C.; Zimmermann, W. D. *J. Org. Chem.* **1970**, *35*, 2165.
(23) Laube, B. L.; Asirvatham, M. R.; Mann, C. K. *J. Org. Chem.* **1977**, *42*, 670.
(24) Galliani, G.; Rindone, B.; Scolastico, C. *Tetrahedron Lett.* **1975**, 1285.

Received for review March 2, 2000. Revised manuscript received June 12, 2000. Accepted June 21, 2000.

ES001064C